The Journal of Neuroscience, July 1, 2000, *20*(13):4983–4991

Slit Inhibition of Retinal Axon Growth and Its Role in Retinal Axon Pathfinding and Innervation Patterns in the Diencephalon

Thomas Ringstedt,[1] Janet E. Braisted,[1] Katja Brose,[2] Thomas Kidd,[3] Corey Goodman,[3] Marc Tessier-Lavigne,[2] and Dennis D. M. O'Leary[1]

[1]Molecular Neurobiology Laboratory, The Salk Institute, La Jolla, California 92037, [2]Departments of Anatomy, and Biochemistry and Biophysics, University of California, San Francisco, California 94143-0452, and [3]Department of Molecular and Cell Biology, University of California, Berkeley, California 94720

We have analyzed the role of the Slit family of repellent axon guidance molecules in the patterning of the axonal projections of retinal ganglion cells (RGCs) within the embryonic rat diencephalon and whether the slits can account for a repellent activity for retinal axons released by hypothalamus and epithalamus. At the time RGC axons extend over the diencephalon, *slit1* and *slit2* are expressed in hypothalamus and epithalamus but not in the lateral part of dorsal thalamus, a retinal target. *slit3* expression is low or undetectable. The Slit receptors *robo2*, and to a limited extent *robo1*, are expressed in the RGC layer, as are *slit1* and *slit2*. In collagen gels, axon outgrowth from rat retinal explants is biased away from *slit2*-transfected 293T cells, and the number and length of axons are decreased on the explant side facing the cells. In addition, in the presence of Slit2, overall axon outgrowth is decreased, and bundles of retinal axons are more tightly fasciculated. This action of Slit2 as a growth inhibitor of retinal axons and the expression patterns of *slit1* and *slit2* correlate with the fasciculation and innervation patterns of RGC axons within the diencephalon and implicate the Slits as components of the axon repellent activity associated with the hypothalamus and epithalamus. Our findings suggest that *in vivo* the Slits control RGC axon pathfinding and targeting within the diencephalon by regulating their fasciculation, preventing them or their branches from invading nontarget tissues, and steering them toward their most distal target, the superior colliculus.

Key words: axon guidance; axon fasciculation; axon repellents; chemorepellents; robo1*;* robo2*; hypothalamus; retinal ganglion cells*

Visual information is relayed from the eye to the brain via the axons of retinal ganglion cells (RGCs). RGC axons enter the brain at the ventral aspect of the hypothalamus. In rodents, essentially all RGCs project to their midbrain target, the superior colliculus (SC) (Linden and Perry, 1983). En route to the SC, RGC axons grow dorsally over the lateral surface of the diencephalon. A small fraction of RGC axons invade the ventral hypothalamus to form the retinohypothalamic projection (Johnson et al., 1988; Levine et al., 1991, 1994). In contrast, approximately one-third of RGC axons later extend branches into their targets in dorsal thalamus (e.g., the dorsal lateral geniculate nucleus) (Bhide and Frost, 1991).

The first RGC axons reach the ventral hypothalamus in rats on embryonic day 14 (E14), grow over the diencephalon, and reach the SC on E16 (Lund and Bunt, 1976; Bunt et al., 1983; Marcus and Mason, 1995). Later arriving RGC axons continue to grow over the diencephalon for several more days (Tuttle et al., 1998). RGC axons extend over the hypothalamus in a tight fascicle, defasciculate and spread over the surface of their dorsal thalamic targets, and then refasciculate into a tight bundle as they approach epithalamus and turn caudally toward the SC (Fig. 1A) (Tuttle et al., 1998). This pattern of RGC axon growth over the diencephalon correlates with *in vitro* observations that retinal axons can extend over an inhibitory substrate but in a highly fasciculated manner (Bray et al., 1980). Defasciculation of RGC axons over dorsal thalamus likely facilitates their branching and target innervation (Daston et al., 1996). Consistent with these axonal behaviors, we previously showed that *in vitro* the hypothalamus and epithalamus release soluble activities that repel rat and mouse retinal axons, whereas dorsal thalamus releases an activity that promotes their growth (Tuttle et al., 1998) (Fig. 1*B*). The molecular identities of these activities are unknown; however, members of the Slit family of secreted proteins are candidates for the repellent activity.

In *Drosophila*, the transmembrane receptor Roundabout (Robo) is expressed on axons, plays a role in preventing ipsilaterally projecting axons from crossing the midline and commissural axons that have crossed the midline from recrossing (Seeger et al., 1993; Kidd et al., 1998; Zallen et al., 1998). Mutant analysis suggests that Robo is a receptor for a midline repellent activity, subsequently shown to be Slit. In mammals, three *slit* genes, *slit1*, *slit2*, and *slit3*, and two Slit receptors, *robo1* and *robo2,* have been identified (Itoh et al., 1998; Nakayama et al., 1998; Brose et al., 1999; Li et al., 1999). Slit2 has been shown to be a chemorepellent for olfactory bulb, hippocampal (Nguyen Ba-Charvet et al., 1999), and spinal motor axons (Brose et al., 1999). The objective of the present study was to evaluate the role of the Robos and Slits in the patterning of RGC projections within the embryonic rat dien-

Received Feb. 29, 2000; revised April 17, 2000; accepted April 18, 2000.

This work was supported by National Institutes of Health Grant EY07025 (D.D.M.O'L.). C.G. and M.T.L. are Investigators of the Howard Hughes Medical Institute. T.R. is supported by the Swedish Brain Foundation and the Swedish Medical Research Council.

Drs. Ringstedt and Braisted contributed equally to this work

Correspondence should be addressed to Dennis D. M. O'Leary, Molecular Neurobiology Laboratory, The Salk Institute, 10010 North Torrey Pines Road, La Jolla, CA 92037. E-mail: doleary@salk.edu.

 0270-6474/00/204983-09$15.00/0

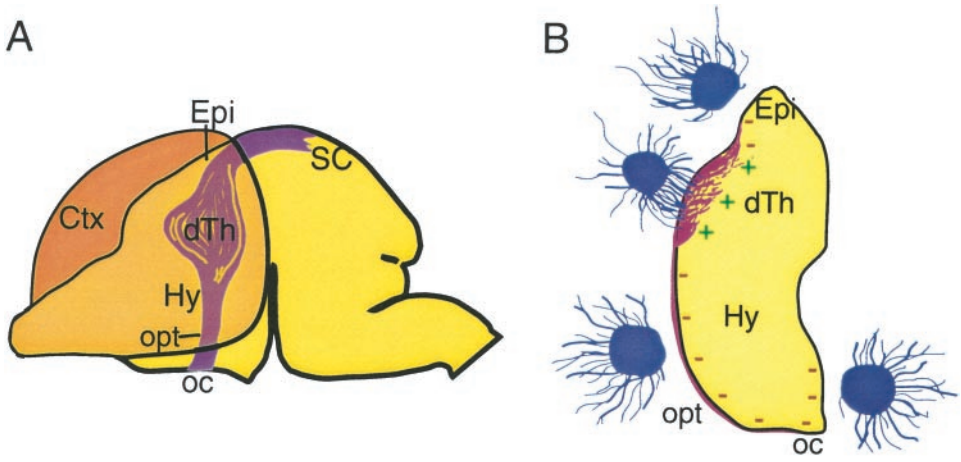

Figure 1. The RGC axon pathway in E17 rat and the distribution of repellent and attractant activities in diencephalon. Schematics of sagittal (*A*) and coronal (*B*) views. For clarity, the cortex is outlined as transparent (*Ctx*, *orange*) in *A* and is not present in *B*. *A*, The optic tract (*opt*) from the optic chiasm (*oc*) to the SC is represented in *purple*. RGC axons are tightly fasciculated as they course over the surface of the hypothalamus (*Hy*) but begin to defasciculate when they reach ventral thalamus, spread out dramatically over the lateral surface of dorsal thalamus (*dTh*), and later form and extend branches into their dorsal thalamic target nuclei (and to a lesser extent ventral thalamus). As RGC axons extend beyond the dorsal thalamus and approach epithalamus (*Epi*), they refasciculate on the surface of diencephalon and turn caudally to grow toward the SC. (Adapted from Tuttle et al., 1998). *B*, Summary of collagen gel coculture studies of Tuttle et al. (1998) that showed that the hypothalamus and epithalamus release soluble repellent activities (represented by − signs), and the lateral part of the dorsal thalamus (i.e., the target nuclei for RGC axons) releases a growth-promoting activity (represented by + signs) for retinal axons. These findings were obtained by coculturing multiple E15 rat retinal explants (*purple*) at a distance from different parts of whole living vibratome coronal sections of E15, E17, or E19 rat diencephalon (dorsal is *up*, and lateral is to the *left*).

cephalon and whether the slits can account for the hypothalamic and epithalamic repellent activities.

MATERIALS AND METHODS

Animals

Sprague Dawley rats from E13 to E17 were obtained from timed-pregnant females (Harlan Sprague Dawley, Indianapolis, IN). Embryos were staged according to Butler and Juurlink (1987). The day of insemination was designated as E0.

In situ *hybridization*. Timed-pregnant rats (E13–E17) were anesthetized with sodium pentobarbital and cesarean-sectioned to expose the embryos. Embryos were decapitated, and the heads were fixed by immersion in 4% paraformaldehyde (Pfa). After cryoprotection (30% sucrose), the heads were coronally sectioned at 20 μm on a cryostat. The sections were fixed for 20 min in 4% Pfa, rinsed twice in PBS, and then delipidated in 2× standard SSC at 65° C for 30 min. After two rinses in water and PBS, the slides were acetylated for 10 min in 0.25% acetic anhydride in 0.1 M ethanolamine and then rinsed in PBS and alcohol-dehydrated. After drying, the sections were incubated overnight in a humidified chamber with 90 ml of hybridization buffer per slide (hybridization buffer is 50% formamide, 10% dextran sulfate, 1× Denhardt's solution, 0.3 M NaCl, 10 mM Tris, pH 7.5, 10 mM sodium phosphate, pH 6.8, and 5 mM EDTA). Antisense RNA probes were added to a concentration of between 20,000 and 50,000 cpm/μl hybridization buffer. After hybridization, the sections were washed 30 min at 55°C in 5× SSC with 20 mM β-mercaptoethanol (β-me), 30 min in 1× SSC (with 20 mM β-me) at 65°C, 45 min at 65°C in 1× SSC, 50% formamide, and 20 mM β-me, and 2 hr at 37°C in 0.5× SSC, 50% formamide, and 20 mM β-me. They were then treated with RNase A (20 μg/ml) for 30 min at 37°C, washed three times for 15 min in 1× SSC at 60°C and 5 min in 0.2× SSC at room temperature. Finally, sections were dehydrated, dried, and dipped in Kodak (Eastman Kodak, Rochester, NY) NT-B2 emulsion. After 5–8 d, the slides were developed, stained with DAPI (Sigma, St. Louis, MO), and mounted in Permount. Probes were labeled with [^{35}S]UTP by *in vitro* transcription with T7 RNA polymerase from fragments of Slit1, Slit2, Slit3, Robo1, or Robo2 subcloned into PBS S/K (Stratagene, La Jolla, CA).

Preparation of explants

Timed-pregnant rats (E15) were anesthetized with sodium pentobarbital and cesarean-sectioned to expose the embryos. Embryos were decapitated, the eyes were removed, and retinas were dissected from surrounding tissues and cut into eight radially symmetric pieces without regard to the retinal axes. Explants were then cocultured overnight in DMEM–F12 with 2 mM glutamine, 0.1% penicillin–streptomycin, 20 mM HEPES, 0.6% D-glucose, and 10% rat serum (growth medium), supplemented with 10 μM cytosine arabinoside (AraC). Retinal axon growth is greater and more radially symmetric, and non-neuronal cell migration from the explants is reduced in cultures exposed briefly to AraC. At the concentrations and exposure times used here, AraC does not appear to have detrimental effects on neurons (Martin et al., 1990). The following day, explants were rinsed in DMEM–F12 and plated in growth medium without AraC as described below.

Preparation of aggregates of slit2*-transfected cells*

293T cells were transfected with *slit2-myc* cDNA using SuperFect Transfection Reagent (Qiagen, Hilden, Germany). The expression vector was constructed by inserting a sequence encoding human Slit2 into the expression vector pSecTagB. pSecTagB without insert was used for mock transfections. Several days before transfection, confluent 60 mm plates were split 1:10. Subconfluent cells were then transfected as follows: 4 μg of DNA was diluted into DMEM to a final volume of 150 μl, and then 20 μl of SuperFect Transfection Reagent was added to the DNA solution. The samples were incubated for 5–10 min before adding 1 ml of DMEM with 0.1% penicillin–streptomycin and 10% FBS (cell growth medium). Cell growth medium was removed from the cells and replaced with the transfection solution. Two to 3 hr later, the transfection solution was removed, the cells were rinsed three times with PBS, and then 5 ml of cell growth medium was added to the dishes. After 24 hr, cells were harvested, centrifuged to a pellet, and resuspended in 100–300 μl of cell growth medium (see below). Agar blocks containing cells were then prepared as follows: 2% low melting point agar in DMEM–F12 was added to a 35 mm dish and allowed to gel. A 1 cm square was cut out and removed, and the dish was placed on a warming block. Thirty-five microliters of cells and 35 μl of molten 2% agar in DMEM–F12 was added to this cavity, mixed, and allowed to gel. Small cubes were then cut from the agar and placed in cell growth medium and cultured overnight. Cell blocks were then rinsed in L15–glucose and cut into smaller pieces (~300–400 μm cubes) before plating.

Preparation of collagen gel cocultures

Collagen was prepared from adult rat tails. Cocultures were set up as follows: 900 μl of collagen solution was mixed with 100 μl of 10× MEM and 13–20 μl of a 1 M solution of sodium bicarbonate and placed on ice. Twenty-five microliters of collagen was pipetted onto the bottom of four-well dishes (Nunc, Naperville, IL) and allowed to gel. Retinal explants were then placed onto this base with a Pasteur pipette, excess L15-glucose was removed, and 75 μl of collagen was added on top. With forceps, retinal explants and *slit2-myc*- or vector (mock)- transfected 293T cell aggregates were positioned ~150–300 μm apart. The collagen was then allowed to gel before adding 500 μl of DMEM–F12 containing 0.1% penicillin–streptomycin, 0.6% D-glucose, 2 mM glutamine, and 5% rat serum. Explants were cultured in a humidified 37°C, CO^2 incubator for 1–1.5 d.

Immunocytochemistry

Collagen gel cocultures were fixed for at least 1 d in 4% paraformaldehyde plus 1% glutaraldehyde at 4°C, rinsed numerous times in 0.1 M

phosphate buffer, and then blocked for 2–4 hr in 10% lamb serum in PBS with 0.1% Triton X-100 (blocking buffer). Cocultures were then incubated 3–4 d at 4°C in mouse monoclonal anti-β tubulin antibody (Amersham Pharmacia Biotech, Arlington Heights, IL), diluted 1:500 in blocking buffer, rinsed numerous times in PBS, and incubated in Cy3-conjugated anti-mouse secondary antibody (Amersham Pharmacia Biotech), diluted 1:1000 in blocking buffer for 2 d. Cultures were then rinsed in PBS and stored at 4°C.

Analysis of axon outgrowth in collagen gel cocultures

After fixation, retina 293T cell cocultures were labeled with an anti-β tubulin monoclonal antibody (see above) and photographed using a 4× or 6.3× lens on a Nikon (Tokyo, Japan) Microphot fluorescence microscope. The micrographs were then scanned into Adobe Photoshop (Adobe Systems, San Jose, CA). Quantitation was done on the scanned images. All data were analyzed using Student's *t* test.

Number and length of axon bundles. On each image, a line was drawn through the center of the retinal explant, dividing it in two sectors, one facing toward and one away from the 293T cells (see Fig. 6). Axon bundles were counted in both sectors, and their lengths were measured.

Directional effects. To determine whether retinal axons turn in response to Slit2, the axons angle of deviation away from the 293T cells was measured in the half of the explant facing toward the 293T cells (see Fig. 7*A*) as follows. A base line, perpendicular to the one dividing the explant in two sectors and to the surface of the 293T cells, was drawn. Another line, the expected direction of growth (*Gx*), was drawn through the center of the explant and the base of the axon bundle. A third line, representing the actual direction of growth (*Ga*) was then drawn through the base and the tip of the axon bundle. The absolute value of the angle between the baseline and *Ga* (*AGa*) was then subtracted from the absolute value of the angle between the baseline and *Gx* (*AGx*). The difference is negative when the axon bundle extends away from the 293T cells and positive when it grows toward them.

Fasciculation. Scanned images were transferred into Scion (Frederick, MD) Image (beta 3b). The optical density was measured as average pixel values (0–256) in a circular area centered at a position that corresponded to 75% of the length of the bundle from the explant. The diameter of the circle was adjusted to fit the width of the fascicle. All fascicles in the focal plane were measured, regardless of whether they projected toward or away from the explant. The background value of the image was measured as the average of several areas in the collagen gel at similar distances from the explant but devoid of axon bundles. The bundle values minus the mean background value were averaged for each coculture, and the average per coculture was calculated.

RESULTS

Expression of Slits in diencephalon

To determine whether the Slits may be involved in the controlling the pathfinding and innervation patterns of RGC axons within the diencephalon, we examined the expression patterns of the mammalian slit homologs *slit1*, *slit2*, and *slit3*, relative to the developing RGC axonal pathway. *In situ* hybridizations were performed on coronal sections of E15 and E17 rat brains, ages when RGC axons grow over the diencephalon and a repellent activity for retinal axons is released by the hypothalamus and epithalamus (Tuttle et al., 1998).

At E15, *slit1* is strongly expressed in the ventromedial part of ventral thalamus and throughout much of the hypothalamus, with particularly high levels in the dorsal two-thirds (Fig. 2*A*). *Slit2* is highly expressed in medial ventral thalamus, as well as in discrete areas within the dorsal and ventral regions of hypothalamus (Fig. 2*C*). In addition, *slit1* is expressed weakly (Fig. 2*A*) and *slit2* is expressed strongly (Fig. 2*C*) in epithalamus and just lateral to the dorsal thalamic ventricular zone. Neither *slit1* (Fig. 2*A*) nor *slit2* (Fig. 2*B*) are expressed in the lateral aspect of dorsal thalamus, a target of RGC axons.

At E17, both *slit1* (Fig. 2*B*) and *slit2* (Fig. 2*D*) continue to be highly expressed within the hypothalamus, with *slit2* expression highest in the ventral half. At this age, a small wedge of *slit1* expression is present in the lateral aspect of dorsal thalamus (Fig. 2*B*). In addition, *slit1* is expressed strongly in epithalamus and in a thin band at the midline of dorsal thalamus; *slit2* expression is high in the epithalamic and dorsal thalamic ventricular zones. In contrast, at both E15 (Fig. 2*E*) and E17 (Fig. 2*F*), *slit3* expression in the diencephalon is very low (e.g., ventral hypothalamus and dorsal thalamus, except its lateral aspect) or nondetectable relative to *slit1* and *slit2*.

These expression patterns of the Slits correlate with the fasciculation and innervation patterns of RGC axons within the diencephalon (for description, see Fig. 1). In summary, at the levels of the diencephalon over which the optic tract courses, we find that the combined expression of the Slits is high in the hypothalamus (high fasciculation, restricted sparse innervation), declines to lower levels in the lateral part of ventral thalamus (tract begins to defasciculate, restricted modest innervation), declines further to nondetectable levels throughout most of the lateral part of dorsal thalamus (tract is defasciculated, heavy innervation), and then increases to high levels in the epithalamus (high fasciculation and tract turns caudally, no innervation). These findings are consistent with a role for Slit1 and/or Slit2 as diencephalic repellents for RGC axons.

Expression of Slit receptors in retina

If *slit1* and *slit2* act as repellents for RGC axons, we would expect that *robo1* and/or *robo2*, receptors for the Slits (Brose et al., 1999; Yuan et al., 1999), would be expressed by RGCs. To test this possibility, *in situ* hybridizations were performed on sections through E13, E15, and E17 rat retinas, ages that cover the majority of the period of RGC axon growth.

At all ages examined, *robo1* is expressed most strongly in the retinal marginal zone (Fig. 3*A–C*). In addition, beginning at E15, scattered cells in the RGC layer in central retina are well labeled (Fig. 3*B*,*G*). By E17, *robo1* expression is present at low levels throughout the retina, with punctate dense labeling in the forming RGC layer, indicative of scattered highly expressing cells (Fig. 3*C*). *robo2* is expressed in central retina at E13, with especially high levels on the vitreal side, the location of the forming RGC layer (Fig. 3*E*,*D*). Expression of *robo2* spreads peripherally such that at E17 *robo2* is expressed throughout the retina, again with highest expression in the forming RGC layer (Fig. 3*F*,*H*).

These data demonstrate that, at the time RGC axons are extending over the diencephalon, *robo2*, and to a lesser extent *robo1*, receptors for Slit1 and Slit2, are expressed in the RGC layer. Given the high, uniform expression of *robo2* in the RGC layer, we conclude that most if not all RGCs express it. However, because only a small proportion of cells in the RGC layer highly express *robo1*, it is difficult to be certain that they are RGCs because a sizeable proportion of cells in the adult RGC layer are displaced amacrine cells (Jeon et al., 1998). In summary, our findings suggest that Slit1 and/or Slit2, acting predominantly through Robo2, may act as diencephalic repellents for RGC axons *in vivo*.

Expression of Slits in retina

We also examined the expression of *slit1*, *slit2*, and *slit3* within the retina at E13, E15, and E17. At all ages examined, both *slit1* (Fig. 4*A–C*) and *slit2* (Fig. 4*D–F*) are most highly expressed in the RGC layer. Expression is first detected at E13 in central retina but spreads peripherally over time, apparently following the central to peripheral gradient of the generation of RGCs (Morest, 1970). In addition, a domain of high *slit2* expression surrounds RGC axons coursing through the optic nerve (Fig. 4*E*,*F*). In

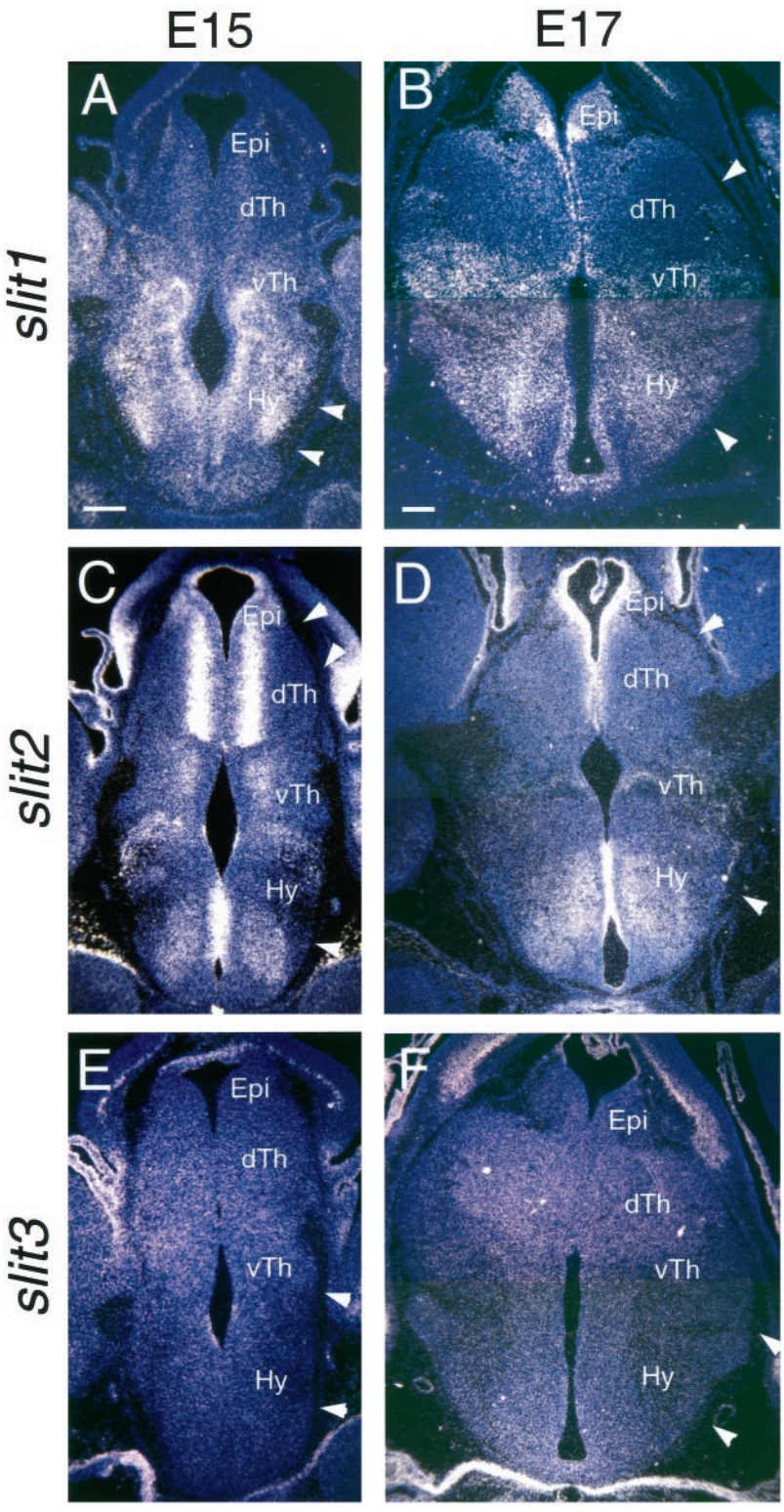

Figure 2. Expression of the *slits* in embryonic rat diencephalon. Coronal sections through the diencephalon of E15 (*A*, *C*, *E*) and E17 (*B*, *D*, *F*) rat brains showing *slit1* (*A*, *B*), *slit2* (*C*, *D*), and *slit3* (*E*, *F*) expression detected with S^{35}-labeled riboprobes. Dorsal is *up*. Sections were stained with bisbenzimide. Each photo is a single exposure using both dark-field and UV fluorescence illumination. *A*, At E15, *slit1* is expressed in the ventromedial part of ventral thalamus, as well as throughout the dorsal two-thirds of hypothalamus. *slit1* expression is also detected in medial dorsal thalamus and epithalamus. *B*, At E17, *slit1* continues to be expressed throughout most of hypothalamus, as well as in medial ventral and dorsal thalamus, and epithalamus. *C*, At E15, *slit2* is highly expressed in medial dorsal thalamus and at lower levels in epithalamus, medial ventral thalamus, and in distinct parts of dorsal and ventral hypothalamus. *D*, At E17, *slit2* is most highly expressed in the dorsal thalamic, epithalamic, and ventral hypothalamic ventricular zones, as well as throughout ventral hypothalamus. In contrast, *slit3* is expressed at low or nondetectable levels in diencephalon at both E15 (*E*) and E17 (*F*). *Arrowheads* mark the optic tract. Scale bars, 200 μm.

contrast, *slit3* (Fig. 4*G–I*) is not expressed to any significant degree in the retina at any of the ages examined. At E17, *slit1* exhibits a graded, high ventral to low dorsal expression pattern. These data suggest that *in vivo*, Slit1 and Slit2, acting predominantly through Robo2, and to a lesser extent through Robo1, may be involved in intraretinal development. In addition, if both Robo and Slit proteins are present on RGC axons, they might modulate interactions between RGC axons.

Slit2 biases and inhibits retinal axon growth in collagen gels

To determine the effects of Slit2 on RGC axon growth, we cocultured in three-dimensional collagen gels explants of retina at a distance from aggregates of 293T cells transiently transfected with *slit2-myc* cDNA or with vector cDNA as a control. Similar analyses were not done for Slit1 because we have not been able to produce sufficient levels of Slit1 protein by transfection. Explants

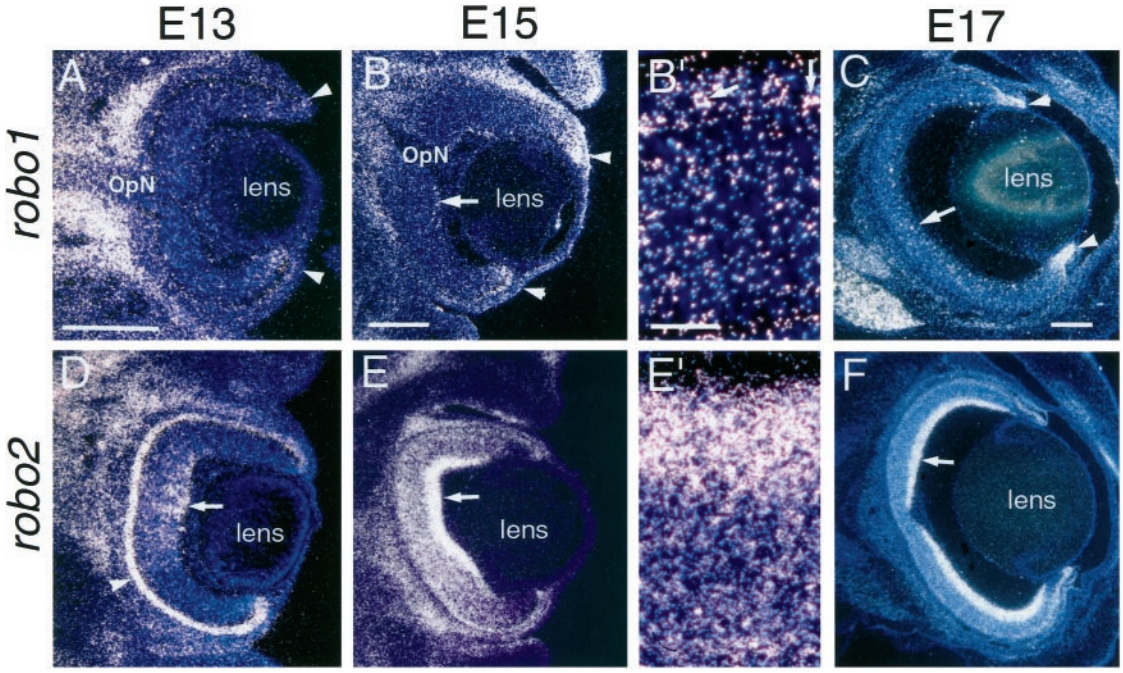

Figure 3. Expression of the Slit receptors, *robo1* and *robo2*, in embryonic rat retina. Coronal sections of E13 (*A*, *D*), E15 (*B*, *B′*, *E*, *E′*), and E17 (*C*, *F*) rat retinas showing *robo1* (*A–C*) and *robo2* (*D–F*) expression detected with S^{35}-labeled riboprobes. Dorsal is *up*. The sections are counterstained with bisbenzimide. Each photo is a single exposure using both dark-field and UV fluorescence illumination. *B′* and *E′* are higher power views of the regions marked with an *arrow* in *B* and *E*, respectively. At 13 (*A*), E15 (*B*, *B′*), and E17 (*C*), *robo1* is expressed in the retinal marginal zone (*arrowheads*). Scattered cells that appear to be highly expressing *slit1* are detected in the ganglion cell layer in central retina at E15 (*arrows* in *B*, *B′*) and at E17 (*arrow* in *C*). At E13 (*D*) and E15 (*E*, *E′*), *robo2* is expressed in central retina, with highest levels in the ganglion cell layer (*arrows*). It is also highly expressed in the epithelium at E13 (*D*, *arrowhead*). At E17, *robo2* is expressed throughout the retina, with highest levels in the ganglion cell layer (*arrow* in *F*). *OpN*, Optic nerve. Scale bars, 200 μm.

of retina were prepared from E15 rat embryos, an age when RGC axons are extending over the diencephalon *in vivo* and are responsive to the hypothalamic and epithalamic repellent activities *in vitro* (Tuttle et al., 1998).

Axon outgrowth from retinal explants is robust when cocultured with mock-transfected cells (Fig. 5*A–D*), whereas when cocultured with *slit2*-transfected cells (Fig. 5*E–H*), outgrowth is substantially decreased. Overall, axon growth appears to be biased away from the cells, and often bundles of axons originate on the explant side facing the *slit2*-transfected cells (Fig. 5*G*). We quantified several features of axon outgrowth in the cocultures, including the bias in outgrowth, the length of axon bundles, and the total number of axon bundles, using the scheme presented in Figure 6*A*. When retina is cocultured with mock-transfected cells ($n = 18$), 35% more axon bundles extend from the side facing toward the cells compared with the side away from them (Fig. 6*B*). In contrast, when retina is cocultured with *slit2*-transfected cells ($n = 20$), 30% fewer axon bundles emanate from the side facing toward the cells (Fig. 6*B*). Comparison between the two types of cocultures reveals that the ratio of toward to away is decreased by ~50% in the Slit2 cocultures. Thus, Slit2 substantially alters the distribution of axon outgrowth from retinal explants, resulting in a biased outgrowth away from the source of Slit2. In addition, Slit2 results in a decrease in the length of retinal axon bundles. In cocultures with mock-transfected cells, axon bundles are the same length on the explant sides toward and away from the cells, whereas in the Slit2 cocultures, they are 35% shorter on the side toward the *slit2*-transfected cells compared with the away side (Fig. 6*C*). This decrease in the length of axon bundles suggests that Slit2 slows the rate of retinal axon extension.

The overall axon outgrowth from retinal explants is also diminished in the presence of *slit2*-transfected cells. Counts of the total number of axon bundles emanating from retinal explants in the cocultures shows that the number is decreased by 84% in the cocultures with *slit2*-transfected cells compared with mock-transfected cells (Fig. 6*D*). Thus, Slit2 is a potent inhibitor of retinal axon growth *in vitro*. The growth inhibition of Slit2 appears to be concentration-dependent because, on the explant side facing the *slit2*-transfected cells in which the amount of Slit2 protein should be greater, fewer axon fascicles emerge (Fig. 6*B*) and they are shorter (Fig. 6*C*).

Although retinal axon outgrowth is fasciculated in both sets of cocultures, the axon bundles generally appear to be denser, that is more tightly fasciculated, in the presence of Slit2 (Fig. 5). To assess the degree of fasciculation, we digitally measured the optical density of the axon bundles immunostained using an anti-β-tubulin antibody, with the rationale being that more tightly fasciculated axon bundles should exhibit a greater optical density (see Materials and Methods). Retinal explants cocultured with mock-transfected cells had an average pixel value of 100 ± 1.5 (on a scale of 0 to 256), whereas those cocultured with *slit2*-transfected cells had an average pixel value of 114.7 ± 5.9. This difference was highly significant ($p < 0.005$; Student's *t* test). We therefore conclude that retinal axons are more tightly fasciculated in the presence of Slit2.

The findings described above demonstrate that Slit2 inhibits retinal axon growth and alters the distribution of outgrowth from retinal explants, resulting in a biased growth away from the source of Slit2. To determine whether Slit2 also has a directional affect on retinal axon growth, especially whether it repels retinal axons, we measured the angle of deviation of axons away from

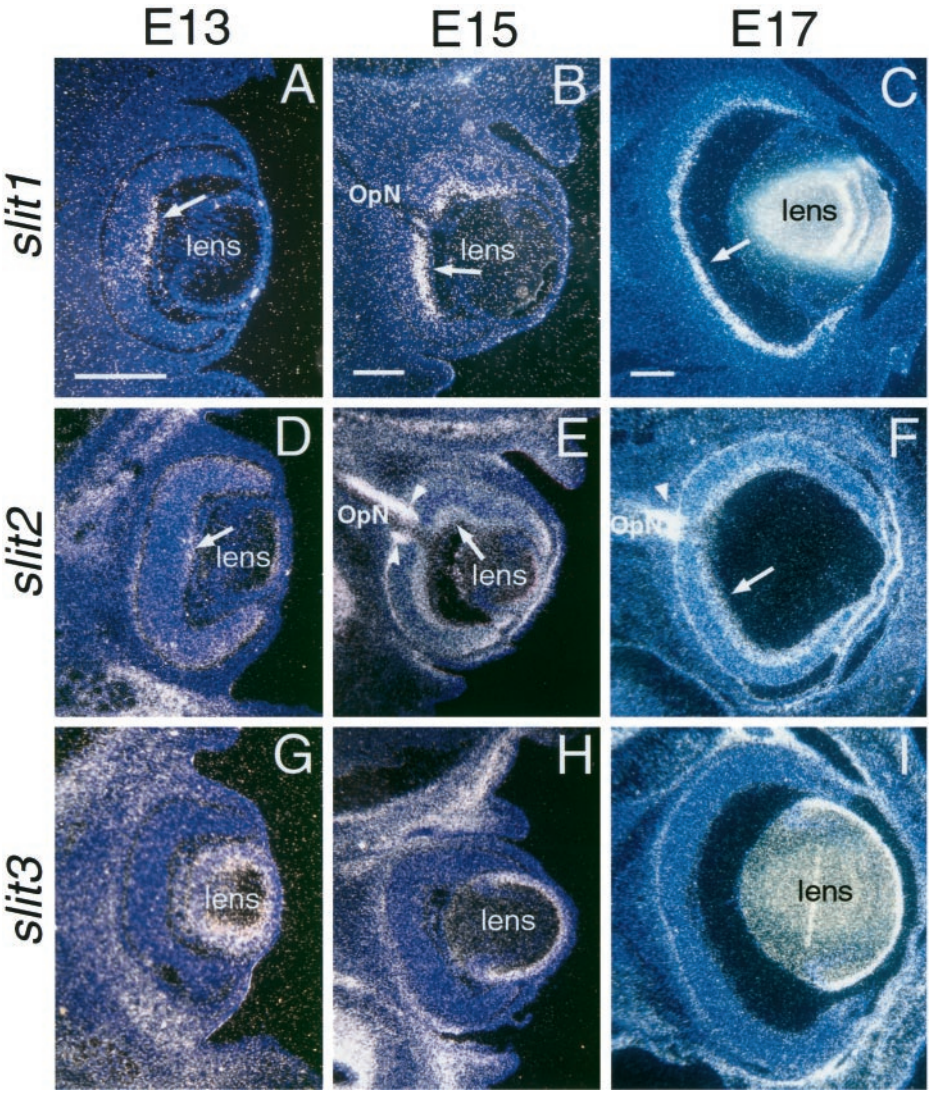

Figure 4. Expression of Slits in embryonic rat retina. Coronal sections of E13 (*A*, *D*, *G*), E15 (*B*, *E*, *H*), and E17 (*C*, *F*, *I*) rat retinas showing *slit1* (*A–C*), *slit2* (*D–F*), and *slit3* (*G–I*) expression detected with S^{35}-labeled riboprobes. Dorsal is *up*. The sections are counterstained with bisbenzimide. Each photo is a single exposure using both dark-field and UV fluorescence illumination. At E13 (*A*, *D*) and E15 (*B*, *E*), *slit1* (*A*, *B*) and *slit2* (*D*, *E*) expression is highest in the ganglion cell layer in central retina (*arrows*), but by E17, both *slit1* (*C*) and *slit2* (*F*) are expressed throughout the RGC layer (*arrows*). Note that *slit1* expression is more restricted to the ganglion cell layer than *slit2* expression. *Arrowheads* in *E* and *F* indicate expression of *slit2* at the optic disk and bounding the optic nerve (*OpN*). *slit2* expression at E17 shows a high ventral to low dorsal graded pattern (*C*). *slit3* expression is not detected in retina at E13 (*G*), E15 (*H*), or E17 (*I*). Scale bars, 200 μm.

slit2-transfected cells (Fig. 7*A*). We found no significant difference in axon turning when retinal explants are cocultured with *slit2*-transfected compared with mock-transfected cells (Fig. 7*B*). Thus, although Slit2 biases and inhibits retinal axon growth *in vitro*, we are lacking formal criteria that Slit2 is also a chemorepellent for retinal axons.

DISCUSSION

Our previous work showed that the hypothalamus and epithalamus release a soluble repellent activity for rat and mouse retinal axons and that the distribution of this activity correlates with the fasciculation and innervation patterns of RGC axons within the embryonic diencephalon (Tuttle et al., 1998). Here, we presented evidence that the axonal chemorepellents Slit1 and Slit2 comprise the diencephalic repellent activity. At the time RGC axons extend over the diencephalon, *slit1* and *slit2* are expressed in the hypothalamus and epithalamus but not in RGC target nuclei in dorsal thalamus, and most if not all RGCs express the Slit receptor *robo2,* and a limited number might express *robo1*. In addition, our *in vitro* assays show that Slit2 is a potent inhibitor of retinal axon growth. These findings, together with those of Erskine et al. (2000) and Niclou et al. (2000), suggest that the slits have crucial roles in RGC axon pathfinding from the eye to the midbrain.

Within the retina, we find that the Robo receptors and *slit1* and *slit2* are coexpressed in the RGC layer, with *slit1* exhibiting a high ventral to low dorsal graded expression. Other axon guidance ligands and receptors are also coexpressed in the retina, often in a graded manner in the RGC layer, including EphA and EphB receptors and their ephrin-A and ephrin-B ligands (Cheng et al., 1995; Kenny et al., 1995; Marcus et al., 1996; Braisted et al., 1997; Holash et al., 1997; Monschau et al., 1997). The graded expression of the ephrin-A ligands appears to regulate the pool of functional EphA receptors on RGCs via receptor phosphorylation and influence RGC axon guidance by enhancing the gradient of functional receptors (Connor et al., 1998; Hornberger et al., 1999). Although the role of the coincident expression of the Slits and Robos in RGCs is undefined, it may serve to modulate axon–axon interactions within the RGC axon pathway and thereby influence the fasciculation of RGC axons and their responses to Slits expressed along the pathway (see below).

It seems likely that *robo2* is the primary mediator of RGC axon response to the Slits, because it is expressed at much higher levels in the RGC layer than *robo1*. However, the relative contributions

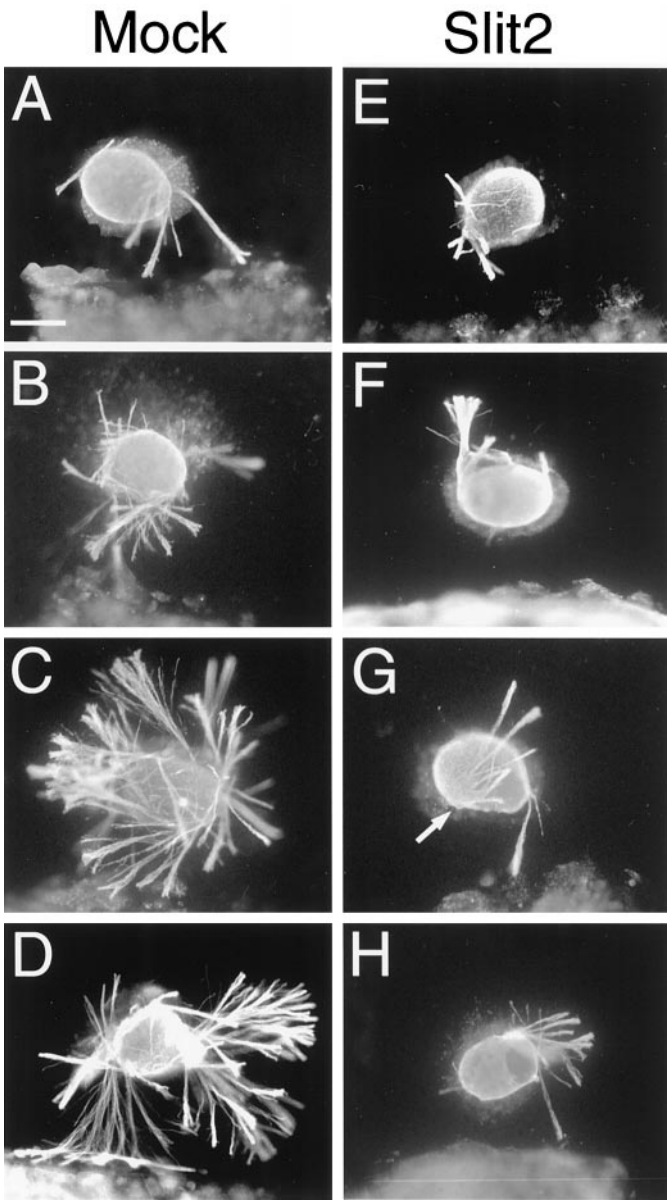

Figure 5. Axon outgrowth from retinal explants is biased away from, and inhibited by, *slit2*-transfected cells. Explants from E15 rat retinas were cocultured for 1–1.5 d in collagen gels at a distance from aggregates of 293T cells transfected with human *slit2-myc* (*Slit2*) or, as a control, with the parental plasmid (*Mock*). Cocultures were immunostained with an anti-β-tubulin antibody (see Materials and Methods) and photographed under fluorescence illumination. The 293T cells are to the *bottom*. Shown are a representative series of explants to show the range and bias of axon outgrowth. *A–D*, When cocultured with mock-transfected cells, retinal axon outgrowth is robust and exhibits a modest bias toward the cells. All 18 explants had outgrowth in the mock cocultures. *E–H*, In contrast, when cocultured with *slit2*-transfected cells, retinal axon outgrowth is substantially decreased and is biased away from the cells. Five of 20 explants in the Slit2 cocultures had no outgrowth (data not shown). The *arrow* in *G* marks axon bundles that arise from the side of the explant facing the *slit2*-transfected cells but extend away for them. Scale bar, 200 μm.

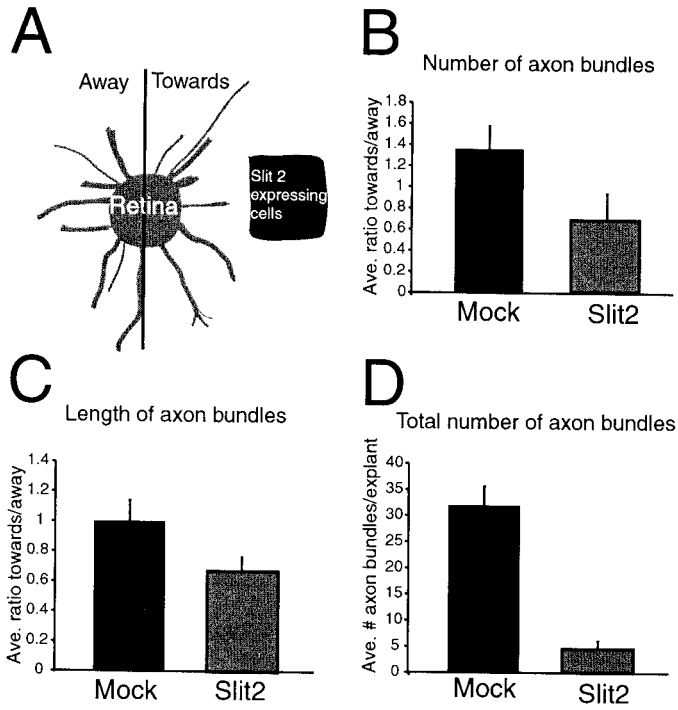

Figure 6. Quantification of effects of Slit2 on biasing and inhibiting retinal axon outgrowth *in vitro*. *A*, Quantitation scheme. Cocultures were labeled with an anti-β-tubulin antibody, and the number and length of axon bundles were quantified in the hemiretina sector facing toward or away from the 293T cells. Quantitation was done blind to transfected cell type on 18 cocultures with mock-transfected 293T cells (575 axon bundles) and 20 cocultures with *slit2*-transfected 293T cells (92 axon bundles). *B*, Axon outgrowth is biased away from *slit2*-transfected cells. The ratio of the number of axon bundles extending from the explant side facing the 293T cells compared with the side facing away from the cells is decreased by ~50% in the retina Slit2 compared with the retina mock cocultures ($p < 0.04$; Student's *t* test). *C*, Axon length is decreased by Slit2. The ratio of the length of axon bundles on the side of the explant facing toward compared with the side facing away from the cells is decreased by ~35% in the retina Slit2 compared with the retina mock cocultures ($p < 0.05$; Student's *t* test). *D*, Slit2 decreases overall axon outgrowth. The total number of axon bundles extending from retinal explants is decreased by 84% in the retina Slit2 compared with the retina mock cocultures ($p < 4 \times 10^{-9}$; Student's *t* test).

of Slit1 and Slit2 in influencing RGC axon growth within the diencephalon is less clear. We have shown that Slit2 inhibits retinal axon growth and is expressed in the hypothalamus and epithalamus at the time RGC axons extend over the diencephalon. *slit1* is also highly expressed in the hypothalamus and epithalamus in a pattern that partially overlaps with that of *slit2*, but thus far we have not tested its function. However, Slit1 is a repellent for olfactory axons (Yuan et al., 1999) and migrating olfactory progenitor cells (Wu et al., 1999). Therefore, it is likely that both Slit1 and Slit2 are components of the hypothalamic and epithalamic repellent activities.

The expression patterns of *slit1* and *slit2*, and our findings that RGC axon growth is both inhibited and more tightly fasciculated in the presence of slit2, relate well to the fasciculation and innervation patterns of RGC axons within the diencephalon. RGC axons are tightly bundled and invade sparsely if at all parts of the diencephalon that express the slits, i.e., the hypothalamus and epithalamus, and are defasciculated and innervate parts that do not express the slits, i.e., their target nuclei in the lateral part of dorsal thalamus. The fasciculation pattern of the RGC axons in relation to domains of ;slit expression is consistent with the demonstration that retinal axons are able to extend over an inhibitory substrate *in vitro* but in a highly fasciculated manner (Bray et al., 1980). Thus, one possible role for the Slits expressed in the hypothalamus and epithalamus is to promote the fascicu-

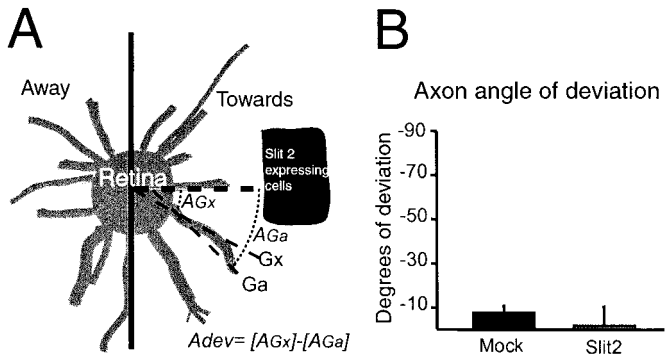

Figure 7. Quantitation of the effect of Slit2 on the directional growth of retinal axons *in vitro*. *A*, Quantitation scheme. Quantitation was done blind to transfected cell type on 13 randomly selected cocultures of each type (those with no outgrowth were not used); 575 axon bundles were analyzed in the cocultures with mock-transfected cells, and 32 axon bundles were analyzed in the *slit2*-transfected cell cocultures. The axons angle of deviation away from the 293T cells was measured in the "toward" hemiretina sector as follows: a line (*Gx*), representing the expected direction of growth, was drawn through the center of the explant and the base of the axon bundle. A second line (*Ga*), representing the actual direction of growth, was then drawn through the base and the tip of the axon bundle. The absolute value of the angle between the base line (*thick dashed line*) and *Ga* (*AGa*) was then subtracted from the absolute value of the angle between the baseline and *Gx* (*AGx*). The difference is negative when the bundle extends away from the 293T cells and positive when it extends toward them. *B*, Retinal axons are not repelled by Slit2 in collagen gel cocultures. No significant difference is found in the angle of deviation of axon bundles away from the 293T cells between the retina mock and the retina Slit2 cocultures ($p = 0.22$; Student's t test).

lation of RGC axons. The defasciculation of RGC axons over dorsal thalamus may be allowed by its lack of Slit expression and could be enhanced by a Slit-mediated repulsion between RGC axons because RGCs appear to express Robos and Slits. The potential action of the Slits on RGC axon fasciculation may be similar to the influences of the ephrin-A axonal repellents on the fasciculation of cortical axons (Winslow et al., 1995) and retinal axons (McLaughlin and O'Leary, 1999).

Because the hypothalamus expresses *slit1* and *slit2*, it may seem counterintuitive that RGC axons enter the brain at its ventral aspect and extend dorsally over its surface. It is likely though that the Slit-mediated inhibition is balanced by activities that promote and direct RGC axon growth, for example the chemoattractant netrin-1 (De la Torre et al., 1997; Deiner et al., 1997). This idea is supported by analyses of RGC axon pathfinding in mice deficient for the homeodomain protein Vax1 (Bertuzzi et al., 1999). *vax1* is expressed in discrete populations of cells of the optic stalk, nerve and chiasm, and ventral hypothalamus. In *vax1* mutants, RGC axons fail to form a chiasm and very few penetrate the brain. Instead, at their entry point in ventral hypothalamus, RGC axons form a "Probst-like" bundle that is capped by an aberrant dense cluster of cells, which are normally $vax1^+$. Thus, a domain that is normally growth permissive for RGC axons, is inhibitory in the mutants: a change that correlates with a dramatic decrease in *netrin-1* expression but maintained expression of *slit1* (Bertuzzi et al., 1999). Similarly, *netrin-1* expressed at the optic disk and in the optic nerve may neutralize any inhibitory effects on RGC axon growth exerted by Slit2 expressed at the optic disk and bounding the nerve (Fig. 3*E*,*F*), which may help explain why the optic nerve is reduced or absent in *netrin-1* mutant mice (Deiner et al., 1997). In normal development, the expression of *slit2* surrounding the optic nerve may serve to channel RGC axons from the eye to the brain.

RGCs innervate their targets via branches that form along RGC axons at specific locations within the optic tract (Bhide and Frost, 1991; Simon and O'Leary, 1992a,b). Our findings suggest that the Slits may prevent RGC axons from forming and extending branches into nontarget tissues. This could be achieved in two ways. First, the Slits could directly inhibit branch formation and extension, similar to apparent role of ephrin-A in inhibiting retinal axon branching (Roskies and O'Leary, 1994; O'Leary et al., 1999). This action is the opposite of that of the N-terminal fragment of Slit2, which promotes the elongation and branching of dorsal root ganglia axons *in vitro* (Wang et al., 1999). A second way would be a result of Slit-mediated modulation of axon fasciculation; the defasciculation of RGC axons over dorsal thalamus should facilitate their branching and innervation of their target nuclei, whereas their branching over the hypothalamus should be diminished by their tight fasciculation. This suggestion is supported by the finding that the branching of corticospinal axons is delayed and diminished by the selective removal of polysialic acid from their surfaces, which results in an increase in their fasciculation (Daston et al., 1996).

As RGC axons approach the domain of *slit1* and *slit2* expression in the epithalamus, they not only refasciculate but also turn and grow caudally toward the SC, suggesting that the Slits may act *in vivo* as repellents for RGC axons. Although our *in vitro* data indicate that Slit2 inhibits retinal axon growth, our analysis of axon turning failed to provide evidence that Slit2 is a chemorepellent for retinal axons. Although we previously referred to the unidentified hypothalamic and epithalamic activities as repellents for retinal axons (Tuttle et al., 1998), we did not perform a quantitative analysis of axon turning as we have done for Slit2. However, we did find that retinal axon growth is biased away from the hypothalamus and epithalamus *in vitro*, similar to our finding here that retinal axon growth is biased away from *slit2*-transfected cells. Although our data do not reveal a directional, i.e., repellent, effect of Slit2 on retinal axons, the Slits might nonetheless act *in vivo* as repellents and promote RGC axon turning. We suspect that axon turning in the collagen cocultures is impeded by the fasciculation of rat retinal axons, which is enhanced in the presence of Slit2. This situation has similarities to the effect of chemoattractant netrin-1 on spinal commissural axons: although netrin-1 can cause the turning of spinal axons under some conditions *in vitro* (Kennedy et al., 1994; Hong et al., 1999), in collagen gels it induces the outgrowth of axon bundles but does not affect their directionality (Kennedy et al., 1994).

We conclude that Slit1 and Slit2 play a role in the pathfinding of RGC axons and the patterning of their projections within the diencephalon by regulating the fasciculation of RGC axons within the optic tract, preventing them or their branches from invading nontarget tissues and steering them toward their distal target, the SC. It will be of interest to determine the requirement of the Slits for the development of RGC projections and to identify other molecules that cooperate with the Slits to define the path of RGC axons through the diencephalon and promote their innervation of their dorsal thalamic targets.

REFERENCES

Bertuzzi S, Hindges R, O'Leary DDM, Lemke G (1999) The homeodomain protein Vax1 is required for axon guidance and development of major axon tracts in the brain. Genes Dev 13:3092–3105.

Bhide PG, Frost DO (1991) Stages of growth of hamster retinofugal

axons: implications for developing axonal pathways with multiple targets. J Neurosci 11:485–504.
Braisted JE, McLaughlin T, Wang HU, Friedman GC, Anderson DJ, O'Leary DDM (1997) Graded and lamina-specific distributions of ligands of EphB receptor tyrosine kinases in the developing retinotectal system. Dev Biol 191:14–28.
Bray D, Wood P, Bunge RP (1980) Selective fasciculation of nerve fibres in culture. Exp Cell Res 130:241–250.
Brose K, Bland KS, Wang KH, Arnott D, Henzel W, Goodman CS, Tessier-Lavigne M, Kidd T (1999) Slit proteins bind Robo receptors and have an evolutionarily conserved role in repulsive axon guidance. Cell 96:795–806.
Bunt SM, Lund RD, Land PW (1983) Prenatal development of the optic projection in albino and hooded rats. Dev Brain Res 6:149–168.
Butler H, Juurlink BHJ (1987) An atlas for staging mammalian and chick embryos. Boca Raton, FL: CRC.
Cheng HJ, Nakamoto M, Bergemann AD, Flanagan JG (1995) Complementary gradients in expression and binding of ELF-1 and Mek4 in development of the topographic retinotectal projection map. Cell 82:371–381.
Connor RJ, Menzel P, Pasquale EB (1998) Expression and tyrosine phosphorylation of Eph receptors suggest multiple mechanisms in patterning of the visual system. Dev Biol 193:21–35.
Daston MM, Bastmeyer M, Rutishauser U, O'Leary DDM (1996) Spatially restricted increase in polysialic acid enhances corticospinal axon branching related to target recognition and innervation. J Neurosci 16:5488–5497.
De la Torre JR, Hopker VH, Ming GL, Poo MM, Tessier-Lavigne M, Hemmati-Brinvalou A, Holt CE (1997) Turning of retinal growth cones in a netrin-1 gradient mediated by the netrin receptor DCC. Neuron 19:1211–1224.
Deiner MS, Kennedy TE, Fazeli A, Serafini T, Tessier-Lavigne M, Sretavan DW (1997) Netrin-1 and DCC mediate axon guidance locally at the optic disc: loss of function leads to optic nerve hypoplasia. Neuron 19:575–589.
Erskine L, Williams SE, Brose K, Kidd T, Rachel RA, Goodman CS, Tessier-Lavigne M, Mason CA (2000) Retinal ganglion cell axon guidance in the mouse optic chiasm: expression and function of Robos and Slits. J Neurosci, in press.
Holash JA, Soans C, Chong LD, Shao H, Dixit VM, Pasquale EB (1997) Reciprocal expression of the Eph receptor Cek5 and its ligand(s) in the early retina. Dev Biol 182:256–269.
Hong K, Hinck L, Nishiyama M, Poo MM, Tessier-Lavigne M, Stein E (1999) A ligand-gated association between cytoplasmic domains of UNC5 and DCC family receptors converts netrin-induced growth cone attraction to repulsion. Cell 97:927–941.
Hornberger MR, Dutting D, Ciossek T, Yamada T, Handwerker C, Lang S, Weth F, Huf J, Wessel R, Logan C, Tanaka H, Drescher U (1999) Modulation of EphA receptor function by coexpressed ephrinA ligands on retinal ganglion cell axons. Neuron 22:731–742.
Itoh A, Miyabayashi T, Ohno M, Sakano S (1998) Cloning and expressions of three mammalian homologues of *Drosophila* slit suggest possible roles for Slit in the formation and maintenance of the nervous system. Brain Res Mol Brain Res 62:175–186.
Jeon CJ, Strettoi E, Masland RH (1998) The major cell populations of the mouse retina. J Neurosci 18:8936–8946.
Johnson RF, Morin LP, Moore RY (1988) Retinohypothalamic projections in the hamster and rat demonstrated using cholera toxin. Brain Res 462:301–312.
Kennedy TE, Serafini T, De la Torre JR, Tessier-Lavigne M (1994) Netrins are diffusible chemotropic factors for commissural axons in the embryonic spinal cord. Cell 78:425–435.
Kenny D, Bronner-Fraser M, Marcelle C (1995) The receptor tyrosine kinase QEK5 mRNA is expressed in a gradient within the neural retina and the tectum. Dev Biol 172:708–716.
Kidd T, Brose K, Mitchell KJ, Fetter RD, Tessier-Lavigne M, Goodman CS, Tear G (1998) Roundabout controls axon crossing of the CNS midline and defines a novel subfamily of evolutionarily conserved guidance receptors. Cell 92:205–215.
Levine JD, Weiss ML, Rosenwasser AM, Miselis RR (1991) Retinohypothalamic tract in the female albino rat: a study using horseradish peroxidase conjugated to cholera toxin. J Comp Neurol 306:344–360.
Levine JD, Zhao XS, Miselis RR (1994) Direct and indirect retinohypothalamic projections to the supraoptic nucleus in the female albino rat. J Comp Neurol 341:214–224.
Li HS, Chen JH, Wu W, Fagaly T, Zhou L, Yuan W, Dupuis S, Jiang ZH, Nash W, Gick C, Ornitz DM, Wu JY, Rao Y (1999) Vertebrate slit, a secreted ligand for the transmembrane protein roundabout, is a repellent for olfactory bulb axons. Cell 96:807–818.
Linden R, Perry VH (1983) Massive retinotectal projection in rats. Brain Res 272:145–149.
Lund RD, Bunt AH (1976) Prenatal development of central optic pathways in albino rats. J Comp Neurol 165:247–264.
Marcus RC, Mason CA (1995) The first retinal axon growth in the mouse optic chiasm: axon patterning and the cellular environment. J Neurosci 15:6389–6402.
Marcus RC, Gale NW, Morrison ME, Mason CA, Yancopoulos GD (1996) Eph family receptors and their ligands distribute in opposing gradients in the developing mouse retina. Dev Biol 180:786–789.
Martin DP, Wallace TL, Johnson Jr EM (1990) Cytosine arabinoside kills postmitotic neurons in a fashion resembling trophic factor deprivation: evidence that a deoxycytidine-dependent process may be required for nerve growth factor signal transduction. J Neurosci 10:184–193.
McLaughlin T, O'Leary DDM (1999) Functional consequences of coincident expression of EphA receptors and ephrin-A ligands. Neuron 22:636–639.
Monschau B, Kremoser C, Ohta K, Tanaka H, Kaneko T, Yamada T, Handwerker C, Hornberger MR, Loschinger J, Pasquale EB, Siever DA, Verderame MF, Muller BK, Bonhoeffer F, Drescher U (1997) Shared and distinct functions of RAGS and ELF-1 in guiding retinal axons. EMBO J 16:1258–1267.
Morest DK (1970) The pattern of neurogenesis in the retina of the rat. Z Anat Entwicklungsgesch 131:45–67.
Nakayama M, Nakajima D, Nagase T, Nomura N, Seki N, Ohara O (1998) Identification of high-molecular-weight proteins with multiple EGF-like motifs by motif-trap screening. Genomics 51:27–34.
Nguyen Ba-Charvet KT, Brose K, Marillat V, Kidd T, Goodman CS, Tessier-Lavigne M, Sotelo C, Chedotal A (1999) Slit2-Mediated chemorepulsion and collapse of developing forebrain axons. Neuron 22:463–473.
Niclou SP, Jia L, Raper JA (2000) Slit2 is a repellent for retinal ganglion cell axons. J Neurosci, in press.
O'Leary DDM, Yates P, McLaughlin T (1999) Mapping sights and smells in the brain: distinct mechanisms to achieve a common goal. Cell 96:255–269.
Roskies AL, O'Leary DDM (1994) Control of topographic retinal axon branching by inhibitory membrane-bound molecules. Science 265:799–803.
Seeger M, Tear G, Ferres-Marco D, Goodman CS (1993) Mutations affecting growth cone guidance in *Drosophila*: genes necessary for guidance toward or away from the midline. Neuron 10:409–426.
Simon DK, O'Leary DDM (1992a) Development of topographic order in the mammalian retinocollicular projection. J Neurosci 12:1212–1232.
Simon DK, O'Leary DDM (1992b) Responses of retinal axons *in vivo* and *in vitro* to position-encoding molecules in the embryonic superior colliculus. Neuron 9:977–989.
Tuttle R, Braisted JE, Richards LJ, O'Leary DDM (1998) Retinal axon guidance by region-specific cues in diencephalon. Development 125:791–801.
Wang KH, Brose K, Arnott D, Kidd T, Goodman CS, Henzel W, Tessier-Lavigne M (1999) Biochemical purification of a mammalian slit protein as a positive regulator of sensory axon elongation and branching. Cell 96:771–784.
Winslow JW, Moran P, Valverde J, Shih A, Yuan JQ, Wong SC, Tsai SP, Goddard A, Henzel WJ, Hefti F, Beck KD, Caras IW (1995) Cloning of AL-1, a ligand for an Eph-related tyrosine kinase receptor involved in axon bundle formation. Neuron 14:973–981.
Wu W, Wong K, Chen J, Jiang Z, Dupuis S, Wu JY, Rao Y (1999) Directional guidance of neuronal migration in the olfactory system by the protein Slit. Nature 400:331–336.
Yuan W, Zhou L, Chen JH, Wu JY, Rao Y, Ornitz DM (1999) The mouse SLIT family: secreted ligands for ROBO expressed in patterns that suggest a role in morphogenesis and axon guidance. Dev Biol 212:290–306.
Zallen JA, Yi BA, Bargmann CI (1998) The conserved immunoglobulin superfamily member SAX-3/Robo directs multiple aspects of axon guidance in *C. elegans*. Cell 92:217–227.